additional intervening protein or proteins. These experiments may have also uncovered an additional role for Est1 in telomerase function, as the Cdc13-Est2 fusion was not capable of promoting extensive telomere elongation in the absence of Est1 (Fig. 3C) (*26*). Because Est1 is a terminus-specific DNA binding protein (*11*), we speculate that this second role may be to promote accessibility of the 3′ terminus to the active site of telomerase.

References and Notes

1. C. I. Nugent and V. Lundblad, *Genes Dev.* **12**, 1073 (1998).
2. J. Shampay and E. H. Blackburn, *Proc. Natl. Acad. Sci. U.S.A.* **85**, 534 (1988).
3. S. Marcand, E. Gilson, D. Shore, *Science* **275**, 986 (1997); B. van Steensel and T. de Lange, *Nature* **385**, 740 (1997); S. Marcand, V. Brevet, E. Gilson, *EMBO J.* **18**, 3509 (1999).
4. C. I. Nugent, T. R. Hughes, N. F. Lue, V. Lundblad, *Science* **274**, 249 (1996).
5. V. Lundblad and J. W. Szostak, *Cell* **57**, 633 (1989).
6. T. S. Lendvay, D. K. Morris, J. Sah, B. Balasubramanian, V. Lundblad, *Genetics* **144**, 1399 (1996).
7. M. S. Singer and D. E. Gottschling, *Science* **266**, 404 (1994).
8. J. Lingner *et al.*, *ibid.* **276**, 561 (1997).
9. M. Cohn and E. H. Blackburn, *ibid.* **269**, 396 (1995).
10. J. Lingner, T. R. Cech, T. R. Hughes, V. Lundblad, *Proc. Natl. Acad. Sci. U.S.A.* **94**, 11190 (1997).
11. V. Virta-Pearlman, D. K. Morris, V. Lundblad, *Genes Dev.* **10**, 3094 (1996).
12. J. J. Lin and V. A. Zakian, *Proc. Natl. Acad. Sci. U.S.A.* **93**, 13760 (1996).
13. B. Garvik, M. Carson, L. Hartwell, *Mol. Cell. Biol.* **15**, 6128 (1995).
14. T. R. Hughes, S. K. Evans, R. G. Weilbaecher, V. Lundblad, in preparation.
15. In-frame fusion proteins were constructed as follows: The Cdc13-Est1 fusion (pVL1091) fused $Cdc13_{1-924}$-$Est1_{6-699}$; the Cdc13-Est2 (pVL1107) and Cdc13-$Est2_{D670A}$ (pVL1111) proteins fused $Cdc13_{1-924}$-$Est2_{1-884}$. All three constructs were expressed from the genomic *CDC13* promoter and derived from the single-copy *CEN* plasmid, pRS415. The Est1-DBD_{Cdc13} and Est1-47-DBD_{Cdc13} fusions (pVL1120 and pVL1121, respectively), expressed in single copy from the *EST1* promoter, fused the Cdc13 DNA binding domain (*22*) to the COOH terminus of Est1, to generate $Est1_{1-699}$ - $Cdc13_{2-21,452-693}$. Telomere elongation by any of these fusion proteins is not due to increased protein expression in the context of the fusion, because overexpression of Est1, Est2, or Cdc13, or expression of Est1 by the *CDC13* promoter, has little or no effect on telomere length (*8*, *11*, *17*, *19*).
16. We have also observed up to a ~4-kb increase in the length of a single telomere (chromosome IIIL). Strains with greatly elongated telomeres do not exhibit any discernable growth defect but were not examined for more subtle defects (such as alterations in cell cycle progression). We have not investigated yet whether the increase in telomere length in strains carrying Cdc13-telomerase fusions occurs at a constant rate, or if there is some influence of cis-inhibition on elongation, as previously observed (*3*).
17. S. K. Evans and V. Lundblad, unpublished data.
18. The *est1-47* mutation is one of a panel of alanine-scan mutations in *EST1* (*17*); the Est1-47 mutant protein still retains association with telomerase (at 20% of WT levels), as assessed by coimmunoprecipitation with the TLC1 RNA (*27*).
19. N. Grandin, S. I. Reed, M. Charbonneau, *Genes Dev.* **11**, 512 (1997).
20. A. Chandra, T. R. Hughes, V. Lundblad, unpublished data.
21. C. I. Nugent, E. Pennock, V. Lundblad, unpublished data.
22. T. R. Hughes, R. G. Weilbaecher, V. Lundblad, in preparation.
23. Previous work showed that high-level expression of the $Est2_{D670A}$ mutant protein (under the control of the *ADH* promoter, on a 2μ high-copy plasmid) resulted in substantially shorter telomeres in an *EST2*$^+$ strain (*8*). The lack of an effect of the Cdc13-$Est2_{D670A}$ fusion on WT telomere length (Fig. 3A) is presumably a consequence of the lower levels of this fusion protein (confirmed by protein immunoblotting analysis), due to single-copy plasmid expression by the *CDC13* promoter. As expected, the Cdc13-$Est2_{D670A}$ fusion failed to complement an *est2*-Δ strain.
24. Bypass of *est1*-Δ senescence was not simply a consequence of increased Est2 levels (due to possible minimal increase in expression of *EST2* by the *CDC13* promoter), because even higher level expression of *EST2* by the constitutive *ADH* promoter (*8*) was not sufficient to allow an *est1*-Δ strain to grow (*17*).
25. V. Lundblad and E. H. Blackburn, *Cell* **73**, 347 (1993).
26. Association of Cdc13-Est2 fusion protein with the TLC1 RNA was reduced by less than twofold in the absence of Est1, as assessed by immunoprecipitation (*27*), arguing that the failure to elongate telomeres in an *est1*-Δ strain is not simply due to reduced stability of the Cdc13-Est2 telomerase complex.
27. For each sample, cells were grown in selective media to an optical density (600 nm) of 1.0. Cells were harvested by centrifugation and the cell pellets were washed in water and then in TMG 300+ [10 mM tris-HCl (pH 8.0), 1 mM $MgCl_2$, 5% glycerol, 1 mM phenylmethylsulfonyl fluoride, 300 mM NaCl]. Cell extracts were prepared by five repeated cycles of freezing and grinding in liquid nitrogen. Extracts were cleared twice by centrifugation for 10 min at 14,000 rpm at 4°C and immunoprecipitated with an antibody to hemagglutinin (HA) (16β12, Babco) and protein A/G agarose beads (Calbiochem). RNA was prepared by SDS–phenol-chloroform extraction, and TLC1 was detected on 7 M urea–4% polyacrylamide gel as described (*8*). The efficiency of TLC1 recovery in immunoprecipitates is typically less than 2%; the recovery with untagged proteins was less than 0.05%.

28. We thank T. Hughes, R. Weilbaecher, and L. Zumstein for critical review of the manuscript. Supported by NIH grant RO1GM55867 (V.L.) and by a U.S. Army Breast Cancer Research Predoctoral Traineeship (S.K.E.).

9 June 1999; accepted 30 August 1999

Protamine-Induced Condensation and Decondensation of the Same DNA Molecule

Laurence R. Brewer,[1] Michele Corzett,[2] Rod Balhorn[2]

The DNA in sperm and certain viruses is condensed by arginine-rich proteins into toroidal subunits, a form of packaging that inactivates their entire genome. Individual DNA molecules were manipulated with an optical trap to examine the kinetics of torus formation induced by the binding of protamine and a subset of its DNA binding domain, Arg_6. Condensation and decondensation experiments with λ-phage DNA show that toroid formation and stability are influenced by the number of arginine-rich anchoring domains in protamine. The results explain why protamines contain so much arginine and suggest that these proteins must be actively removed from sperm chromatin after fertilization.

Protamine and other polycations have been shown to coil DNA into toroidal structures containing up to 60 kb of DNA (*1–3*). Individual bacteriophage appear to contain a single toroid folded inside the protein capsid (*3*), whereas a sperm cell contains as many as 50,000 toroids packed inside its nucleus (*1*). The protamines responsible for inducing torus formation and packaging DNA in maturing spermatids contain a series of arginine-rich anchoring domains (*4*) that bind to the phosphodiester backbone of DNA in a base sequence–independent fashion (*5*). One protamine molecule is bound to each turn [~11 base pairs (bp)] of DNA (*5, 6*), and adjacent arginines in the anchoring domains interlock both strands of the helix. Arginine-rich sequences are also present in the proteins that package DNA in several viruses (*7*), but the viral proteins contain fewer anchoring domains per molecule.

In vitro studies using light scattering (*8, 9*), electron and atomic force microscopy (*1, 2, 10*), fluorescence microscopy (*11, 12*), and DNA elasticity measurements (*13*) have examined how protamine and other polycations induce torus formation. The interpretation of light-scattering experiments has been complicated by DNA aggregation, whereas electron and atomic force microscopy studies characterized only the structure of the final product. Toroid formation and the kinetics of the condensation process could not be observed by fluorescence microscopy because the molecules were not sufficiently extended. To examine toroid formation under conditions that preclude aggregation and precipitation and allow a detailed analysis of kinetics, we used an optical trap to isolate individual DNA molecules and fluorescence microscopy to monitor the formation of toroids in real time

[1]Electronics Engineering Technologies Division, [2]Biology and Biotechnology Research Program, Lawrence Livermore National Laboratory, Livermore, CA 94550, USA.

as they are induced by protamine (or Arg_6) binding.

λ-phage DNA concatemers (20 to 80 μm long) were tagged at one end with a biotinylated oligonucleotide attached to a 1-μm streptavidin-coated polystyrene bead and stained with the intercalating dye YOYO-1 (*14*). These molecules were introduced through one port of a "bifurcated flow cell" (Fig. 1A) and the condensing agent protamine (or Arg_6) through another port so that the two solutions flowed side by side with minimal mixing. An infrared optical trap (*15*) (Fig. 1B) was used to move an individual DNA molecule, via its attached bead, from the sample (DNA) side to the condensing agent (protein) side of the flow cell. The molecule was extended by the force of the flowing buffer, and its entire length became visible because of the fluorescence of the intercalated dye. Toroid formation (condensation) (Fig. 1C) was monitored in real time by measuring the change in length of the molecule as a function of time after moving it into the buffer stream containing protein (*16*).

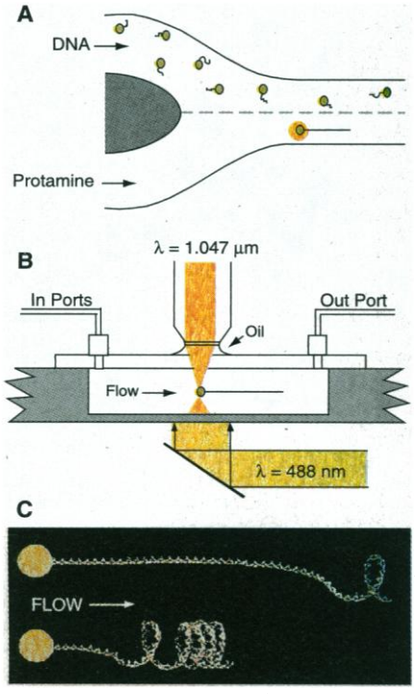

Fig. 1. (**A**) Top view of the flow cell (*25*) showing how the DNA molecules (attached to beads) and protamine enter the cell and form an interface (– – –) with little or no mixing. (**B**) Side view of the system showing the optical trap (orange) holding a bead attached to a single DNA molecule. The cell is illuminated from beneath by a 1-mW argon-ion laser, λ = 488 nm, to excite the YOYO-1 dye bound to the DNA. (**C**) Model of a DNA molecule condensing in protamine (protamine molecules not shown). The upper molecule shows the initiation of coiling and the lower molecule depicts the progression of coiling to form the torus.

Images documenting the progression of condensation for a 50-μm DNA concatemer in protamine (*17*) are shown in Fig. 2. The toroid, which appeared as a bright spot at the end of the DNA molecule, increased in brightness as it moved toward the bead. In 1.1 μM protamine, the condensation process was completed in ~19 s. The change in length versus time for four different DNA molecules as they condensed in different concentrations of protamine is shown in Fig. 3A. As long as the DNA was extended by flow, torus formation initiated at the free end of the molecule, and its length decreased linearly with time, as predicted by Ostrovsky and Bar-Yam (*18*). The movement of the toroid often exhibited a jerky, start-and-stop motion, but when the process was repeated with the same DNA molecule (Fig. 4) this motion was not reproduced. Although these sporadic fluctuations in condensation rate cannot be DNA sequence or conformation dependent, they may relate to the cooperative nature of protamine binding and a nonrandom, incomplete coverage of the DNA molecule that develops as the protamines bind. Condensation (toroid movement) should decrease or stop if the toroid encountered regions that were not completely covered by protamine.

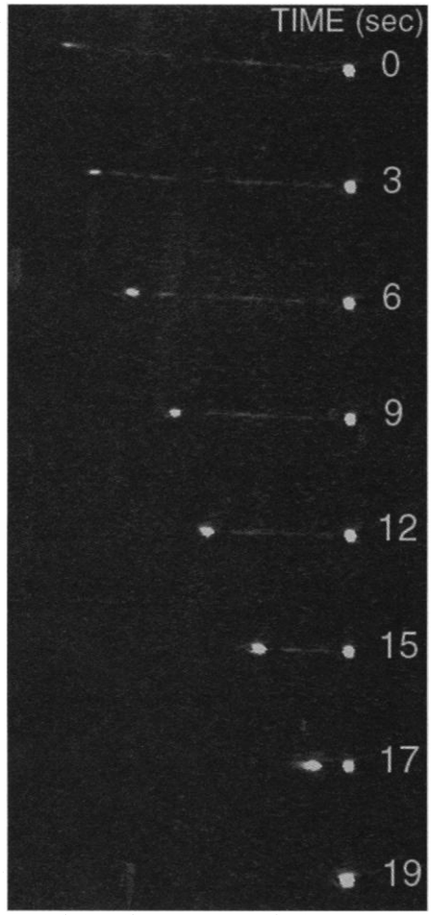

Fig. 2. Progression of condensation of a 50-μm concatemer of λ-phage DNA attached to a 1-μm bead. The bead was held stationary by an optical trap and the DNA molecule is extended by the flow of the incoming buffer containing 1.1 μM protamine (v = 17.6 μm/s). Each time frame was captured after initiation of condensation as shown.

Experiments conducted at different protamine concentrations showed that the rate of condensation was limited by the rate of protamine binding to the DNA molecule. The change in rate (Fig. 3B) was linear, with a slope of 2.6 ± 0.47 μm/μM-s. This corresponds to a rate of protamine binding to DNA of 600 ± 110 molecules/μM-s. The rate of condensation was measured at two different concentrations of YOYO-1 (0.1 and 0.02 μM) to determine whether intercalated YOYO-1 molecules affect the condensation rate. No statistically significant difference in the rates was observed. The potential effect of buffer flow and its frictional force on toroid movement was also assessed by calculating the force that would be exerted on a sphere of equivalent volume to the toroid and by performing an experiment to test the effect of the force directly. The force was calculated by Stokes' law to be 0.43 pN (*19*). The effect of the force was determined experimentally by comparing the condensation rates measured for 30 DNA molecules condensed in 1.5 μM protamine over a range of buffer flow rates (20 to 70 μm/s). The slope of the fitted line through the data points (0.00 ± 0.038) indi-

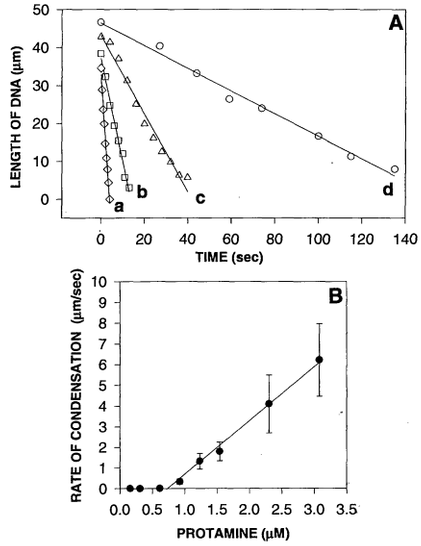

Fig. 3. (**A**) Change in length versus time measured for four different DNA molecules condensed in a different protamine concentration (flow speed, v = 50 μm/s): (**a**) 3.1 μM (diamonds); (**b**) 1.6 μM (squares); (**c**) 1.2 μM (triangles); (**d**) 0.93 μM (circles). Lines are least-squares fits to the data points. (**B**) Condensation rates were determined by collecting data for about 200 individual DNA molecules condensed by protamine.

cated that the condensation rate was not affected by the velocity of the buffer flow.

To estimate the off-rate of protamine, we measured the decondensation rates of individual condensed DNA molecules after moving them back to the DNA side of the flow cell. We monitored decondensation, which occurs only when protamine dissociates from the DNA, for periods up to 25 min and used the lengthening (uncoiling) of the molecule to estimate the rate of protamine dissociation. The measured rate of increase in DNA length, 3.1 ± 1.3 nm/s, corresponds to a protamine off-rate of 0.71 molecule per second (*20*). At this rate, the complete dissociation of protamine from the sperm genome (1.5×10^9 bp) would require at least 6 years. Because sperm chromatin takes only 5 to 10 min to decondense after fertilization, these results support the hypothesis that protamine must be actively removed from DNA (*21*) once the chromatin enters the egg's cytoplasm. The protamine dissociation constant derived from these measurements, 1.17 ± 0.53 nM, is similar to values obtained by others for herring protamine (1.25 nM and 1.15 nM) with bulk DNA (*9, 22*).

Similar studies conducted with Ac-RRRRRR-amide (Arg_6), one of three Arg_6 anchoring domains present in protamine, revealed that a 68-fold higher concentration of Arg_6 (160 μM) was required to achieve a condensation rate comparable to that measured for protamine (4.2 ± 1.1 μm/s). This suggests that either Arg_6 has a much lower binding affinity for DNA, or the consecutive binding of three individual Arg_6 molecules is statistically much less likely than the binding of a single protamine molecule. In contrast to the protamine complexes, DNA molecules condensed by Arg_6 decondensed rapidly when pulled back across the interface and out of the buffer containing the peptide. Four successive condensation-decondensation measurements performed on the same molecule in 107 μM Arg_6 are shown in Fig. 4. The mean condensation rate for these four measurements was 9.1 ± 2.5 μm/s, and the mean decondensation rate was 21.25 ± 2.9 μm/s. Because the Arg_6 molecule binds to only 3 bp of DNA, these data indicate that the off-rate for Arg_6 is 18×10^3 molecules per second—four orders of magnitude higher than the off-rate of protamine (*23*). The dissociation constant, 0.25 ± 0.08 mM, has not been measured previously.

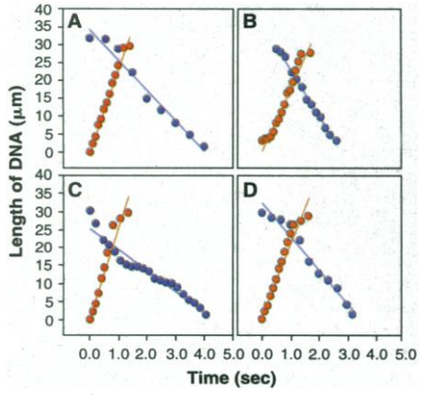

Fig. 4. Condensation (blue dots) and decondensation (red dots) of the same DNA molecule in 107 μM Arg_6 (flow speed, v = 28 μm/s) performed four successive times (**A** to **D**).

Experiments conducted with concatemers of different lengths also indicated that there may be a limit to the amount of DNA that can be coiled into a toroid. Only one toroid was observed during the condensation of single λ-phage DNA molecules, whereas multiple toroids (Fig. 5) were observed when concatemers containing two to four molecules were condensed at a low flow rate (v < 10 μm/s). Although additional experiments must be conducted to verify the maximum length of sequence that can be coiled into a torus, the present studies suggest that one torus is formed for each length of λ-phage DNA (48.5 kb). Although it is not clear why such a limit should exist, this estimate (~50 kb) is close to the 60 kb derived from toroid volumes measured by electron microscopy (*10*).

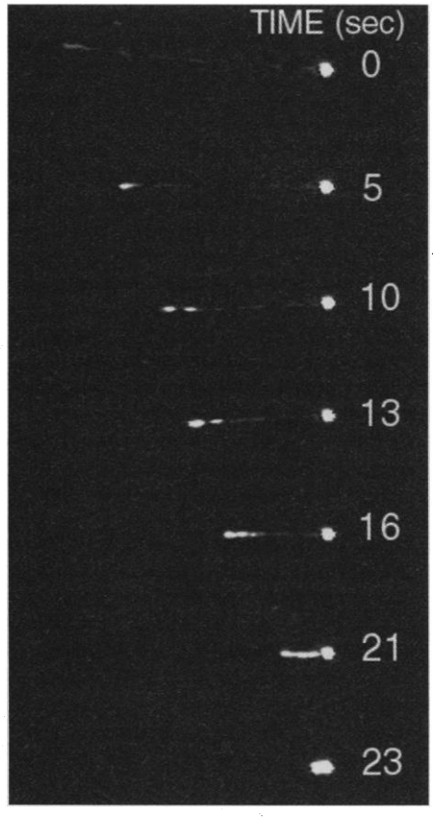

Fig. 5. Condensation of a 45-μm concatemer of λ-phage DNA attached to a 1-μm bead held stationary by an optical trap in 1.1 μM protamine (flow speed, v = 6.1 μm/s). Three toroids were observed to form, sequentially starting at the free end of the DNA molecule.

By combining the use of an optical trap, a dual-port flow cell, and single molecule imaging, we have examined the condensation kinetics of individual DNA molecules, obtained estimates of the binding and dissociation rates for protamine and Arg_6 in the absence of competing aggregation reactions, and monitored the formation and motions of toroids in real time to obtain results that only single molecule studies can provide. In addition to providing new insight into the mechanism of DNA condensation by protamine, this work presents an example of how experiments with single DNA molecules can be used to study the kinetics and biophysics of protein-DNA interactions.

References and Notes

1. N. V. Hud, M. J. Allen, K. H. Downing, J. Lee, R. Balhorn, *Biochem. Biophys. Res. Commun.* **193**, 1347 (1993).
2. R. Balhorn *et al.*, in *The Male Gamete: From Basic Science to Clinical Applications*, C. Gagnon, Ed. (Cache River Press, Vienna, IL, 1999), pp. 55–70.
3. K. E. Richards, R. C. Williams, R. Calender, *J. Mol. Biol.* **78**, 255 (1973); S. M. Klimenko, T. I. Tikchonenko, V. M Andreev, *ibid.* **23**, 523 (1967); N. V. Hud, *Biophys. J.* 69, 1355 (1995).
4. R. Balhorn, in *Molecular Biology of Chromosome Function*, K. W. Adolph, Ed. (Springer-Verlag, New York, 1989), p. 366.
5. N. V. Hud, F. P. Milanovich, R. Balhorn, *Biochemistry* **33**, 7528 (1994).
6. G. S. Bench, A. M. Friz, M. H. Corzett, D. H. Morse, R. Balhorn, *Cytometry* **23**, 263 (1996).
7. T. M. Cao, M. T. Sung, *Biochem. Biophys. Res. Commun.* **108**, (1982); S. Maeda, S. G. Kamita, H. Kataoka, *Repeat. Virol.*, **180**, 807 (1991).
8. J. Widom and R. L. Baldwin, *J. Mol. Biol.* **144**, 431(1980); C. B. Post and B. H. Zimm, *Biopolymers* **21**, 2139 (1982); D. Porschke, *J. Mol. Biol.* **222**, 423 (1991).
9. F. Watanabe and G. Schwartz, *J. Mol. Biol.* **163**, 485 (1983).
10. P. G. Arscott, A. Li, V. A. Bloomfield, *Biopolymers* **30**, 619 (1990); V. A. Bloomfield, *ibid.* **44**, 269 (1998).
11. C. Bustamante, *Annu. Rev. Biophys. Biophys. Chem.* **20**, 415 (1991).
12. M. Ueda and K. Yoshikowa, *Phys. Rev. Lett.* **77**, 2133 (1996).
13. C. G. Baumann, S. B. Smith, V. A. Bloomfield, C. Bustamante, *Proc. Natl. Acad. Sci. U.S.A.* **94**, 6185 (1997).
14. λ-phage DNA molecules were labeled by annealing and ligating a 5′-biotin-labeled 12-base oligonucleotide (Genosys Biotechnologies Inc.) to the cos site. Concatemers of various lengths were formed by annealing unlabeled λ-phage DNA to the biotin-labeled DNA. The biotinylated DNA (2.2 μg) was attached to 1.8×10^8, 1-μm streptavidin beads (Interfacial Dynamics) in 100 mM $NaHCO_3$ (pH 8) at 37°C for 1 hour. The DNA-bead preparation was diluted to 0.2 μg/ml with degassed 50% (w/v) sucrose, 100 mM $NaHCO_3$ (pH 8), 30 mM dithiothreitol (DTT), 0.1 μM YOYO-1 (one dye molecule per 4 to 5 bp of DNA) and incubated for 2 hours before use. Salmon protamine (Sigma) was purified by high-pressure liquid chromatography and lyophilized. Arg_6 (SynPeP) was used as provided. The proteins were dissolved in 50% sucrose containing 100 mM $NaHCO_3$ (pH 8), diluted each day to the required concentrations in degassed 50% sucrose, 100 mM $NaHCO_3$ (pH 8), 30 mM DTT, and stored under nitrogen.
15. The optical trap was formed by focusing laser light from a solid-state Nd-YLF laser (λ= 1.047 μm, Spectra-Physics) through a Zeiss ×100 Plan Neofluor, oil immersion, infinite conjugate, objective. A Zeiss Ax-

ioplan microscope was modified by removing the illumination optics to allow entry of the laser. The typical laser power used to form the trap (exiting the microscope objective) was 50 mW.
16. The fluorescence was detected with an image-intensified charge-coupled device camera (PAULTEK), the signal was recorded on an SVHS VCR, and an Argus Image Processor (Hamamatsu) and a frame grabber (National Instruments PCI 1402) were used to perform background subtraction. The lengths of the DNA molecules, measured between the center of the 1-μm bead and the free end of the molecule, were obtained from frame-grabbed images. The length of stained DNA (48.5 kb) extended by flow was measured to be 19.2 ± 0.82 μm at a flow rate of 72 μm/s in 50% sucrose. Under these conditions, DNA is 93% extended (*24*).
17. The salmon protamine used in these experiments contains 21 positively charged arginines distributed throughout the length of the protein (32 amino acids).
18. B. Ostrovsky and Y. Bar-Yam, *Biophys. J.* **68**,1694 (1995).
19. Stokes' law, $f = 6\pi\eta rv$, where η is the buffer viscosity (15.4 cp), r is the sphere radius, and v is the buffer velocity (50 μm/s), was used to calculate the frictional force on the fully formed toroid. The toroid used to calculate the frictional force had a 90-nm outer diameter and a 30-nm inner diameter and was 20 nm thick (*1*).
20. Because we cannot confirm that every protamine has dissociated from the decondensed DNA molecule, these experiments provide only a maximum value for the off-rate.
21. S. A. Ruiz-Lara, L. Cornudella, A. Rodriguez-Campos, *Eur. J. Biochem.* **240**, 186 (1996).
22. M. Nakano *et al.*, *J. Biochem.* **105**, 133 (1989).
23. With an off-rate this high, molecules containing a single Arg_6 domain would remain bound to the sperm genome for only 2 hours. This is too short a period of time, because the protamine must remain bound to DNA and maintain the sperm chromatin in an inactive state for up to 2 weeks before fertilization.
24. T. T. Perkins, D. E. Smith, R. G. Larson, S. Chu, *Science* **268**, 83 (1995).
25. The flow cell contains two channels, each pumped at the same speed with a single syringe pump. The depth of the flow cell was 40 μm and the molecule was typically held 20 μm beneath the coverslip. Flow velocities were maintained at ~50 μm/s. Using a computer-controlled stage with 0.1-μm resolution to manipulate the position of the flow cell relative to the optical trap, we moved the DNA molecule to the protein side of the flow cell to initiate condensation.
26. Work was performed at Lawrence Livermore National Laboratory (LLNL) under the auspices of the U.S. Department of Energy under contract W-7405-ENG-48. Funding was provided by a LLNL Labwide Laboratory Directed Research Development Award. We thank J. Holzrichter, M. Colvin, and M. Cosman for their suggestions, support, and encouragement; J. W. Cosman and C. Barry for help during the early stages of the study; and J. T. Cosman for generating the computer graphics image of DNA.

1 April 1999; accepted 30 August 1999

Imidazole Rescue of a Cytosine Mutation in a Self-Cleaving Ribozyme

Anne T. Perrotta, I-hung Shih, Michael D. Been*

Ribozymes use a number of the same catalytic strategies as protein enzymes. However, general base catalysis by a ribozyme has not been demonstrated. In the hepatitis delta virus antigenomic ribozyme, imidazole buffer rescued activity of a mutant with a cytosine-76 (C76) to uracil substitution. In addition, a C76 to adenine substitution reduced the apparent pK_a (where K_a is the acid constant) of the self-cleavage reaction by an amount consistent with differences in the pK_a values of these two side chains. These results suggest that, in the wild-type ribozyme, C76 acts as a general base. This finding has implications for potential catalytic functions of conserved cytosines and adenines in other ribozymes and in ribonuclear proteins with enzymatic activity.

Transphosphoesterification reactions catalyzed by self-cleaving and self-splicing RNAs (ribozymes) require loss of a proton from the participating 2′- or 3′-hydroxyl group to promote its nucleophilic attack on the cleavage-site or splice-site phosphate (*1*, *2*). Metal ions can assist in this reaction, and metal-ion catalysis is one of several strategies that ribozymes share with protein enzymes (*1*, *2*). Enhanced nucleophilicity of the hydroxyl group could also result from base-catalyzed deprotonation (*1*–*3*). The pK_a values of the nucleoside side chains (pK_a ~ 3.5 to 4.5), however, appear to be too low to provide efficient general acid-base catalysis at physiologic pH (*4*). Although pK_a values can be shifted closer to neutrality in particular RNA structures (*2*, *5*), it has not been demonstrated that an RNA side chain can act as a general base in catalysis (*1*, *2*).

Department of Biochemistry, Box 3711, Duke University Medical Center, Durham, NC 27710 USA.

*To whom correspondence should be addressed. E-mail: been@biochem.duke.edu

The two hepatitis delta virus (HDV) ribozymes are structurally related self-cleaving RNAs (*6*, *7*) that require a 2′-hydroxyl group on the ribose located immediately 5′ of the cleavage site phosphate (*8*) and that generate products containing a 2′,3′-cyclic phosphate and a 5′-hydroxyl group (*9*). Thus, implied is a cleavage mechanism that involves nucleophilic attack of the 2′-hydroxyl or 2′-alkoxide on the cleavage-site phosphorus (Fig. 1). In the HDV ribozymes, a specific cytosine (C75 in the genomic ribozyme, designated γC75, and its counterpart C76 in the antigenomic ribozyme) has been hypothesized to accept the proton from the attacking 2′-hydroxyl group (*10*, *11*).

To establish that the cytosine base at position 76 was essential for cleavage in the antigenomic ribozyme, we tested whether exogenous cytosine could rescue activity of C76 mutants. We introduced mutations at C76 into the PEX1 antigenomic ribozyme sequence (*12*); consistent with previous findings (*13*), self-cleavage activity of C76u and C76g was undetectable under standard conditions (Fig. 2A). At 37°C, the rate constants were down by a factor of 10^6. Cleavage activity of the C76u ribozyme was partially restored when cytosine was added to the reaction mixture (*14*). Rescue of activity by exogenous bases and base analogs has previously been demonstrated in hammerhead ribozymes containing abasic residues (*15*). In those studies, rescue occurred through compensation of structural changes introduced by the abasic residue. To test whether cytosine rescue of the C76u mutant might reflect a catalytic role for the base, we substituted imidazole for cytosine. For C76u and C76g, addition of 200 mM imidazole (pH 7.4) to the reaction mixtures enhanced cleavage activity at least 250- and 25-fold, respectively (Fig. 2A and Table 1). The 3′ product band in these reactions was the same size as the normal 3′ product, which suggests that imidazole-dependent cleavage occurred at the wild-type cleavage site in the 101-nucleotide (nt) precursor. We tested several other buffers, but only imidazole and 4(5)-methylimidazole enhanced cleavage activity (*14*). A divalent cation (Mg^{2+}, Ca^{2+}, or Mn^{2+}) was required for cleavage of all constructs (Fig. 2A) (*16*).

Imidazole would most likely be acting as either a general base (pK_a ~ 7.0) or a nucleophile in the cleavage reaction. If imidazole acted as a nucleophile in a single-displacement reaction, it should show up in one of the products. However, a 2′,3′-cyclic phosphate would be generated if the adjacent 2′-hydroxyl was the nucleophile. Therefore, we characterized the 5′ cleavage product. For this analysis, the sequence 5′ to the cleavage site in both PEX1 and C76u was shortened from 8 to 3 nt. Wild-type and mutant precursor RNAs were 5′-end-labeled and allowed to cleave in the absence and presence of imidazole, respectively. The 5′ cleavage products for both ribozymes comigrated on polyacrylamide gels under denaturing conditions in which short fragments containing 3′(2′)-terminal phosphates were resolved from frag-